

# Packing of Isophthalate Tetracarboxylic Acids on Au(111): Rows and Disordered Herringbone Structures

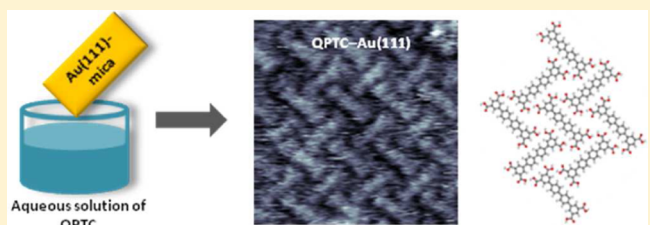
Izabela Cebula,<sup>†,‡,§</sup> Emily F. Smith,<sup>‡</sup> Maria del Carmen Gimenez-Lopez,<sup>‡</sup> Sihai Yang,<sup>‡</sup> Martin Schröder,<sup>‡</sup> Neil R. Champness,<sup>‡</sup> and Peter H. Beton\*,<sup>†</sup>

<sup>†</sup>School of Physics and Astronomy and <sup>‡</sup>School of Chemistry, University of Nottingham, University Park, Nottingham, NG7 2RD, U.K.

<sup>§</sup>Institute of Experimental Physics, University of Wroclaw, Pl. M. Borna 9, 50-204 Wroclaw, Poland

## Supporting Information

**ABSTRACT:** Scanning tunnelling microscopy (STM) has been used to investigate the formation of hydrogen-bonded structures of the isophthalate tetracarboxylic acids, biphenyl-3,3',5,5'-tetracarboxylic acid (BPTC), terphenyl-3,3',5,5'-tetracarboxylic acid (TPTC), and quarterphenyl-3,3',5,5"-tetracarboxylic acid (QPTC), via deposition from solution onto Au(111). STM data reveal that ordered structures can be formed from an aqueous solution leading to the formation of rows for the shortest acid BPTC, while the longer molecules TPTC and QPTC adopt a herringbone-like structure with significant degrees of disorder. The influence of solvent and substrate on the molecular ordering is discussed, and density functional theory is used to identify molecular models for these new phases.



## INTRODUCTION

Carboxylic acids constitute a group of organic molecules which have been extensively explored in surface science and have provided, through studies of the adsorption of trimesic acid on graphite,<sup>1–6</sup> noble metal surfaces<sup>7–11</sup> and dielectric surfaces,<sup>12</sup> some of the first examples of two-dimensional supramolecular assembly. The adsorption of isophthalate tetracarboxylic acids, which have an extra carboxylic acid as compared with trimesic acid, on graphite has been shown to result in the formation of several novel supramolecular arrangements including a random rhombus tiling,<sup>13,14</sup> frustrated crystallization,<sup>15</sup> and guest-induced bilayer growth.<sup>16</sup> These surface studies have so far been limited to investigations of deposition of molecules from solution using alkanoic acids as a solvent, and it is not known whether similar behavior is supported on other substrates, in the presence of other solvents, or, alternatively, for dried films.

We describe in this paper a study aimed at addressing these questions and report herein the formation of adsorbed molecular phases which arise when tetracarboxylic acids are deposited on Au(111) by dipping in an aqueous solution. We observe new surface phases which switch from a parallel to herringbone packing coupled to an intrinsic degree of disorder as the molecular length of the carboxylate is increased. Specifically we investigate biphenyl-3,3',5,5'-tetracarboxylic acid (BPTC), terphenyl-3,3',5,5"-tetracarboxylic acid (TPTC), and quarterphenyl-3,3",5,5"-tetracarboxylic acid (QPTC) (Figure 1).

## EXPERIMENTAL AND THEORETICAL METHODS

(i) Sample preparation: Gold on mica substrates were purchased from Georg Albert PVD (300 nm thick), and

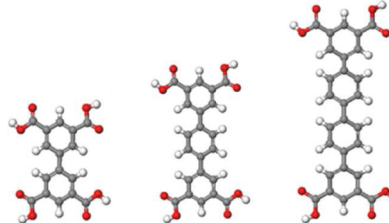


**Figure 1.** Molecular structures of biphenyl-3,3',5,5'-tetracarboxylic acid, BPTC; terphenyl-3,3',5,5"-tetracarboxylic acid TPTC; and quarterphenyl-3,3",5,5"-tetracarboxylic acid, QPTC. Carbon atoms are gray; oxygen atoms red; and hydrogen atoms white.

substrates were flame-annealed using a butane gas torch prior to the deposition of molecules. Freshly annealed Au(111)-mica samples were immediately immersed into aqueous solutions of BPTC (0.5 mM) or TPTC (0.4 mM) or QPTC (0.3 mM) at room temperature. After a few minutes, the samples were removed from the solution and dried in a flow of N<sub>2</sub>. BPTC, TPTC, and QPTC were synthesized using the procedures published previously.<sup>13,17,18</sup>

(ii) STM measurements: All images were obtained using mechanically sharpened PtIr (80:20) wire under ambient conditions on a *Molecular Imaging PicoSPM*. Tunnel current and bias voltages applied to the sample were 50–100 pA and 0.5–0.6 V, respectively.

Received: March 7, 2013

Revised: August 14, 2013

Published: August 14, 2013

(iii) Computational studies: calculations were performed using density functional theory (DFT) using the DMol<sup>3</sup> package in Materials Studio. The effect of the substrate was not included. For input parameters and details for all calculations, see Supporting Information.

## RESULTS

The three carboxylic acids BPTC, TPTC, and QPTC readily adsorb onto the Au(111) surface from an aqueous solution and form phases stabilized by hydrogen bonding. STM images of BPTC, which has the shortest (biphenyl) backbone, on Au(111) are shown in Figure 2. We find that BPTC forms

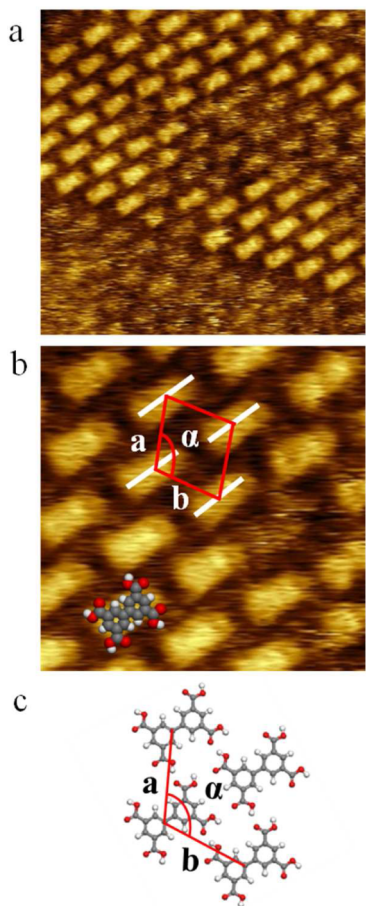


**Figure 2.** STM image of BPTC molecules adsorbed on Au(111): (a)  $12 \times 12 \text{ nm}^2$ , (b) enlarged area of  $5 \times 5 \text{ nm}^2$  showing the measured unit cell (red) and superimposed representation of molecules (white), (c) structural model of BPTC arrangements on a gold surface; experimental and theoretical values of the unit cell parameters are listed in Table 1.

arrays of highly regular rows in which molecules are arranged in a “head-to-tail” arrangement. Surface lattice constants are

identified in Figure 2b, and their values are shown in Table 1. We propose a model, shown in Figure 2c, in which each of the four carboxylic acid groups of the molecule participates in a single hydrogen bond. DFT calculations confirm that the proposed model is stable, and the calculated lattice constants are in excellent agreement with those measured experimentally (Table 1). The binding energy (arising from intermolecular interactions due to hydrogen bonding) per molecule is 0.61 eV. Interestingly there is some freedom associated with this structure since any pair of carboxylic acid groups participating in a hydrogen bond may be rotated by  $180^\circ$  around the bond connecting them to the biphenyl group without significantly modifying the structure. We cannot determine the configuration of the hydrogen bonds from our images, but have confirmed that the unit cell and binding energies remain unchanged when DFT calculations are performed for combinations of molecules with different conformations of carboxylic acid groups (Supporting Information). Thus, the same structural arrangement may accommodate molecules with a range of surface-induced conformation of carboxylic acid groups.

The longer TPTC molecule (Figure 3) does not exhibit row structures but shows a more complex arrangement. The STM images confirm some local order (Figure 3b) in which neighboring molecules are rotated by approximately  $90^\circ$  in a “head-to-edge” arrangement. We have calculated the binding energies of TPTC dimers, and these vary from 0.25 to 0.62 eV per dimer depending on the rotational conformation of the carboxylic acid groups. For example, the dimer with the highest binding energy is shown in Figure 3c. However, images of larger areas show that several other nearest-neighbor configurations occur such as a parallel alignment. Furthermore there is an absence of well-defined domain boundaries, and even within the more ordered regions of the structure, the relative orientation of closely spaced molecules is not identical. These observations imply that there are many possible bonding configurations, and we attribute this to the multiplicity of distinct hydrogen bonding junctions as discussed in the next section.

STM images (Figure 4) of the longest molecule, QPTC, show a nearest-neighbor placement similar to the “head-to-edge” arrangement observed for TPTC. There is a greater degree of order for QPTC, and in this case it is possible to identify separate domains with different orientations and typical dimensions of 10–20 nm, as shown in Figure 4. At the edges of these domains there are disordered regions which are rather similar to those observed for TPTC. From the images we can identify unit cell parameters (Table 1), and the proposed structure is shown in Figure 3c. The stability of this packing arrangement has been confirmed by DFT calculations to give a calculated binding energy of 0.66 eV/molecule and lattice dimensions (Table 1) that are in very good agreement with experimental values.

**Table 1. Comparison of Experimental and Calculated Data Obtained for BPTC, TPTC, and QPTC**

BPTC			TPTC			QPTC		
	STM	DFT		STM	DFT		STM	DFT
a	$1.2 \pm 0.1 \text{ nm}$	$1.18 \pm 0.01 \text{ nm}$	c	$1.2 \pm 0.1 \text{ nm}$	$1.15 \pm 0.01 \text{ nm}$	a	$2.0 \pm 0.2 \text{ nm}$	$2.22 \pm 0.01 \text{ nm}$
b	$1.2 \pm 0.1 \text{ nm}$	$1.18 \pm 0.01 \text{ nm}$	$\beta$	$96 \pm 1^\circ$	$97.2 \pm 0.1^\circ$	b	$1.7 \pm 0.1 \text{ nm}$	$1.63 \pm 0.01 \text{ nm}$
$\alpha$	$106 \pm 2^\circ$	$109.0 \pm 0.1^\circ$		-	-	$\gamma$	$91.0 \pm 0.1^\circ$	$90.3 \pm 0.1^\circ$

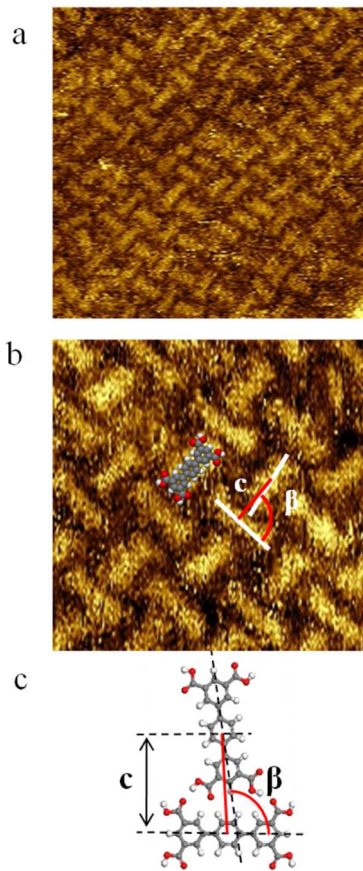


**Figure 3.** STM image of TPTC molecules adsorbed on Au(111): (a)  $15 \times 15 \text{ nm}^2$ , (b) enlarged area of  $7 \times 7 \text{ nm}^2$  showing representation of molecules (white bars) and measured dimensions (red), (c) structural model of TPTC arrangements on a Au(111) surface. Experimental and calculated values of  $c$  and  $\beta$  are given in Table 1.

We have considered the possibility that the molecules are deprotonated following deposition which has previously been reported for related molecules on Cu and Ag surfaces<sup>19–22</sup> under ultrahigh vacuum conditions and following solution deposition. In the current work we do not believe the molecules are deprotonated since the molecular configurations observed in STM images are essentially unchanged for molecules which are deposited from solutions with added sulfuric acid and pH values of 1. In addition we have characterized the molecular layers using X-ray photoelectron spectroscopy (XPS) and found that the peaks in the C 1s and O 1s spectra are in the same positions for monolayers and thick films and are in the positions expected for a protonated carboxylic acid (see Supporting Information).<sup>19–22</sup> In addition previous studies of carboxylic acids on Au(111) have not shown evidence for deprotonation<sup>9</sup> at room temperature, although this effect is reported after annealing.<sup>23</sup>

## ■ DISCUSSION AND CONCLUSIONS

The supramolecular structures we observe display differences in hydrogen bonding junctions between different molecules as compared with previous investigations. For BPTC,<sup>15</sup> TPTC,<sup>13</sup> and QPTC<sup>17</sup> adsorbed on graphite from nonanoic acid (in the presence of the solvent) a double hydrogen bond between adjacent carboxylic acids has been observed, similar to those originally observed for trimesic acid on graphite.<sup>12</sup> For TPTC

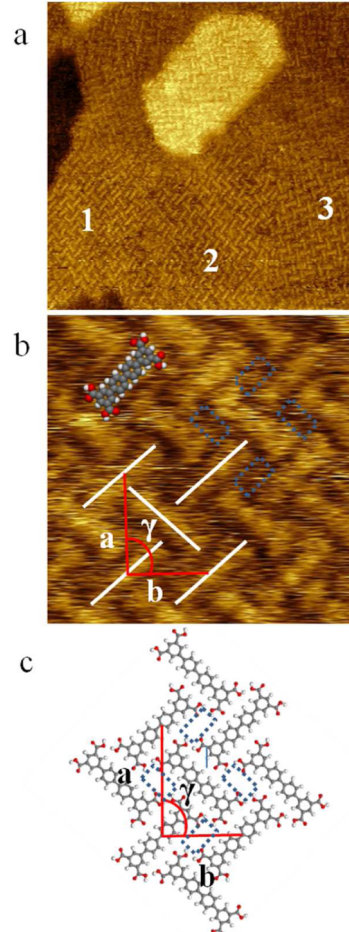


**Figure 4.** STM images of the QPTC adsorbed on Au(111): (a)  $50 \times 50 \text{ nm}^2$  showing different domains (1, 2, 3), (b)  $6 \times 6 \text{ nm}^2$  showing representation of molecules (white bars) and unit cell (red), (c) structural model of QPTC arrangement; experimental and theoretical values of structural parameters are given in Table 1.

and QPTC, the intermolecular binding energy for such a junction has been calculated to be 1.6 eV/molecule, significantly greater than the values calculated in the current work. A common feature of previous studies was the use of nonanoic and other alkanoic acids as solvents, and the resulting supramolecular arrangement is observed to have a more open structure leading to a lower surface density of molecules. For BPTC, TPTC, and QPTC adsorbed on gold we observe molecular densities of 0.7, 0.7, and 0.6 molecules/ $\text{nm}^2$ , respectively. The values for adsorption on graphite are significantly lower: 0.5, 0.4, and 0.3 molecules/ $\text{nm}^2$ , for BPTC, TPTC, and QPTC, respectively. We have recently argued that alkanoic acid molecules stabilize open pore structures on graphite.<sup>14</sup> Thus, for adsorption from nonanoic acid the overall surface energy has contributions from the tetracarboxylic acid molecules, arising from their adsorption to the surface and intermolecular hydrogen bonds, as well as contributions from the adsorption of solvent molecules. Therefore, the differences from the current work can be understood by consideration of the role of a combination of solvent and substrate effects. In the present study, we form monolayers by dipping into an aqueous solution of the carboxylate followed by blow drying, so we would not anticipate that solvent molecules would play a significant role

in the stabilization of the structures we observe. Consequently there is no contribution to the overall surface energy due to solvent adsorption, and the molecules adopt an alternative arrangement in which overall surface energy is minimized through a higher molecular surface density. This higher density leads to a higher overall contribution from the molecule–substrate adsorption energy which we argue compensates for the lower intermolecular energies we see for the current case.

In addition there are interesting differences between each of the molecules studied here. BPTC forms a relatively simple ordered structure over large domains, and as discussed above the intermolecular hydrogen bonding junctions are essentially identical if the carboxylic acid groups are rotated through 180°. This is important since for the tetracarboxylic acids there are two ways to configure each carboxylic acid in a planar adsorption geometry leading to, overall, 2<sup>4</sup> possible surface stabilized configurations for each molecule. Of these, six are equivalent under rotation by 180° about the normal to the surface, leaving 10 surface-induced isomers with inequivalent carboxylic acid configurations. At room temperature rotation of the carboxylic acids is expected to be strongly suppressed for adsorbed molecules so these isomers may not be interconverted. Nevertheless, the calculated degeneracy in intermolecular bonding energy under rotation of carboxylic acid groups indicates that no isomer will be excluded from a BPTC island and can be accommodated next to the suitable nearest neighbor with no additional energy cost. So, despite the likely presence of many isomers, ordered islands can still be formed.

The bonding observed for TPTC has a much more complicated dependence on the orientation of the carboxylic acid groups. The dimer shown in Figure 3 experiences a strong hydrogen bond arising through the interaction of the H atom on the left side of the “head” of the near-vertical molecule and the O atom on the upper-left carboxylic acid of the “edge” horizontal molecule. There is also a significant interaction at the junction between carboxylic acids at the right-hand side of the dimer. Note that the calculated structures are asymmetric with the higher interaction arising from the leftmost junction for the structure shown in Figure 3. Unlike the BPTC molecule, there is a significant dependence of binding energy and dimer geometry under rotation of the two carboxylic acid groups forming this hydrogen bond. This is attributed to additional interactions between O atoms and H atoms attached to the phenyl ring. There is also an additional effect arising from the 180° rotation of the other carboxylic acid group of the vertical molecule. Consequently there are many possible binding energies for the different isomer combinations. These energies range from 0.25 to 0.62 eV with the molecular separation, *c* (see Table 1), ranging from 1.13 to 1.19 nm. The calculations for other carboxylic acid configurations are shown in the Supporting Information. In addition, there are dimers with similar energy with mirror symmetry, but similar geometry, in which the rightmost carboxylic acid junction dominates the intermolecular interaction. Thus, we argue that the multiplicity of many possible bonding junctions between different isomers with small variations in binding energy and geometry provides a source for the disorder which we observe, combined with herringbone-like intermolecular junctions.

For QPTC the intermolecular bonding is rather similar, but a consequence of the slightly longer molecular backbone comprising four phenyl groups is that there is less interplay and dependence of the geometry and binding energy on the configuration of the lower right carboxylic acid group of the

vertical “head” molecule (in analogy with TPTC). In this case, it is possible to build an extended periodic structure from a dimer formed from a single conformational isomer (see Figure 4c). This dimer has a binding energy of 0.33 eV which is close to the lowest calculated energy, 0.39 eV, for all possible dimer junctions. In fact the lowest energy dimer cannot be tessellated into a periodic structure since the respective carboxylic acid groups are not in a configuration which allows this. The close match between the calculated dimensions of all dimers (see Supporting Information) leads us to suggest that the periodic structures contain a mixture of different conformational isomers within the same structural arrangement.

Overall our results highlight the importance of solvent and substrates in preparing such a molecular assembly, and the fragile nature of such structures must be considered when evaluating applications of supramolecular arrays for patterning surfaces. The presence of multiple carboxylic acids within one molecule leads to the possibility of surface-induced conformational and configurational isomers, which must also be considered when determining surface structures. For highly symmetric bonding junctions, such as those observed for these molecules in nonanoic acid, the presence of isomers may be readily accommodated within a single ordered structure. However, for junctions of lower symmetry, as proposed here, the multiplicity of possible junctions can lead to disordered arrangements. The preparation of monolayers by dipping in solutions and subsequent drying is a critical part of the growth of metal organic frameworks (MOFs)<sup>24–26</sup> on surfaces, and our results also provide a basis for future investigations of the tetracarboxylic acids as framework molecules integrated into surface-grown MOFs.

## ■ ASSOCIATED CONTENT

### **S** Supporting Information

Details of the calculations and a full set of calculated structures; XPS results for TPTC on gold; additional large area images for BPTC and TPTC. This material is available free of charge via the Internet at <http://pubs.acs.org>.

## ■ AUTHOR INFORMATION

### **C** Corresponding Author

\*Tel.: +44 115 9515129. E-mail: peter.beton@nottingham.ac.uk.

### **N** Notes

The authors declare no competing financial interest.

## ■ ACKNOWLEDGMENTS

We gratefully acknowledge EPSRC for funding. I.C. thanks LMA Perdigao for assistance with DFT calculations. N.R.C. gratefully acknowledges receipt of a Royal Society Wolfson Merit Award and M.S. of an ERC Advanced Grant.

## ■ REFERENCES

- (1) Griessl, S.; Lackinger, M.; Edelwirth, M.; Hietschold, M.; Heckl, W. M. Self-Assembled Two-Dimensional Molecular Host–Guest Architectures from Trimesic Acid. *Single Mol.* **2002**, *3*, 25–31.
- (2) Lackinger, M.; Griessl, S.; Heckl, W. A.; Hietschold, M.; Flynn, G. W. Self-Assembly of Trimesic Acid at the Liquid–Solid Interface – a Study of Solvent-Induced Polymorphism. *Langmuir* **2005**, *21*, 4984–4988.
- (3) MacLeod, J. M.; Ivasenko, O.; Perepichka, D. F.; Rosei, F. Stabilization of Exotic Minority Phases in a Multicomponent Self-Assembled Molecular Network. *Nanotechnology* **2007**, *18*.

- (4) Griessl, S. J. H.; Lackinger, M.; Jamitzky, F.; Markert, T.; Hietschold, M.; Heckl, W. A. Incorporation and Manipulation of Coronene in an Organic Template Structure. *Langmuir* **2004**, *20*, 9403–9407.
- (5) Ha, N. T. N.; Gopakumar, T. G.; Gutzler, R.; Lackinger, M.; Tang, H.; Hietschold, M. Influence of Solvophobic Effects on Self-Assembly of Trimesic Acid at the Liquid-Solid Interface. *J. Phys. Chem. C* **2010**, *114*, 3531–3536.
- (6) Korolkov, V. V.; Allen, S.; Roberts, C. J.; Tendler, S. J. B. Green Chemistry Approach to Surface Decoration: Trimesic Acid Self-Assembly on HOPG. *J. Phys. Chem. C* **2012**, *116*, 11519–11525.
- (7) Dmitriev, A.; Lin, N.; Weckesser, J.; Barth, J. V.; Kern, K. Supramolecular Assemblies of Trimesic Acid on a Cu(100) Surface. *J. Phys. Chem. B* **2002**, *106*, 6907–6912.
- (8) Li, Z.; Han, B.; Wan, L. J.; Wandlowski, T. Supramolecular Nanostructures of 1,3,5-Benzene-tricarboxylic Acid at Electrified Au(111)/0.05 M H<sub>2</sub>SO<sub>4</sub> Interfaces: An in Situ Scanning Tunneling Microscopy Study. *Langmuir* **2005**, *21*, 6915–6928.
- (9) Ye, Y. C.; Sun, W.; Wang, Y. F.; Shao, X.; Xu, X. G.; Cheng, F.; Li, J. L.; Wu, K. A Unified Model: Self-Assembly of Trimesic Acid on Gold. *J. Phys. Chem. C* **2007**, *111*, 10138–10141.
- (10) Kim, Y.; Cho, K.; Lee, K.; Choo, J.; Gong, M. S.; Joo, S. W. Electric Field-Induced Adsorption Change of 1,3,5-Benzenetricarboxylic Acid on Gold, Silver, And Copper Electrode Surfaces Investigated by Surface-Enhanced Raman Scattering. *J. Mol. Struct.* **2008**, *878*, 155–161.
- (11) Sheerin, G.; Cafolla, A. A. Self-Assembled Structures of Trimesic Acid on the Ag/Si(111)-(√3 x √3)R30 Degrees Surface. *Surf. Sci.* **2005**, *577*, 211–219.
- (12) Rahe, P.; Nimmrich, M.; Kuhnle, A. Substrate Templating upon Self-Assembly of Hydrogen-Bonded Molecular Networks on an Insulating Surface. *Small* **2012**, *8*, 2969–2977.
- (13) Blunt, M. O.; Russell, J. C.; Gimenez-Lopez, M. D.; Garrahan, J. P.; Lin, X.; Schroder, M.; Champness, N. R.; Beton, P. H. Random Tiling and Topological Defects in a Two-Dimensional Molecular Network. *Science* **2008**, *322*, 1077–1081.
- (14) Stannard, A.; Russell, J. C.; Blunt, M. O.; Salesiotis, C.; Gimenez-Lopez, M. D.; Taleb, N.; Schroder, M.; Champness, N. R.; Garrahan, J. P.; Beton, P. H. Broken Symmetry and the Variation of Critical Properties in the Phase Behaviour of Supramolecular Rhombus Tilings. *Nat. Chem.* **2012**, *4*, 112–117.
- (15) Zhou, H.; Dang, H.; Yi, J. H.; Nanci, A.; Rochefort, A.; Wuest, J. D. Frustrated 2D Molecular Crystallization. *J. Am. Chem. Soc.* **2007**, *129*, 13774–13775.
- (16) Blunt, M. O.; Russell, J. C.; Gimenez-Lopez, M. D.; Taleb, N.; Lin, X. L.; Schroder, M.; Champness, N. R.; Beton, P. H. Guest-Induced Growth of a Surface-Based Supramolecular Bilayer. *Nat. Chem.* **2011**, *3*, 74–78.
- (17) Blunt, M. O.; Lin, X.; Gimenez-Lopez, M. D.; Schroder, M.; Champness, N. R.; Beton, P. H. Directing Two-Dimensional Molecular Crystallization Using Guest Templates. *Chem. Commun.* **2008**, *20*, 2304–2306.
- (18) Lin, X.; Telepeni, I.; Blake, A. J.; Dailly, A.; Brown, C. M.; Simmons, J. M.; Zoppi, M.; Walker, G. S.; Thomas, K. M.; Mays, T. J.; et al. High Capacity Hydrogen Adsorption in Cu(II) Tetracarboxylate Framework Materials: The Role of Pore Size, Ligand Functionalization, and Exposed Metal Sites. *J. Am. Chem. Soc.* **2009**, *131*, 2159–2171.
- (19) Lin, N.; Payer, D.; Dmitriev, A.; Strunskus, T.; Woll, C.; Barth, J. V.; Kern, K. Two-Dimensional Adatom Gas Bestowing Dynamic Heterogeneity on Surfaces. *Angew. Chem., Int. Ed.* **2005**, *44*, 1488–1491.
- (20) Stepanow, S.; Strunskus, T.; Lingenfelder, M.; Dmitriev, A.; Spillmann, H.; Lin, N.; Barth, J. V.; Woll, C.; Kern, K. Deprotonation-Driven Phase Transformations in Terephthalic Acid Self-Assembly on Cu(100). *J. Phys. Chem. B* **2004**, *108*, 19392–19397.
- (21) Classen, T.; Lingenfelder, M.; Wang, Y.; Chopra, R.; Virojanadara, C.; Starke, U.; Costantini, G.; Fratesi, G.; Fabris, S.; de Gironcoli, S.; et al. Hydrogen and Coordination Bonding Supra-
- molecular Structures of Trimesic Acid on Cu(110). *J. Phys. Chem. A* **2007**, *111*, 12589–12603.
- (22) Shen, C.; Cebula, I.; Brown, C.; Zhao, J. L.; Zharnikov, M.; Buck, M. Structure of Isophthalic Acid Based Monolayers and Its Relation to the Initial Stages of Growth of Metal–Organic Coordination Layers. *Chem. Sci.* **2012**, *3*, 1858–1865.
- (23) Schwarz, D.; van Gastel, R.; Zandvliet, H. J. W.; Poelsema, B. In Situ Observation of a Deprotonation-Driven Phase Transformation: 4,4'-Biphenyldicarboxylic Acid on Au(111). *J. Phys. Chem. C* **2013**, *117*, 1020–1029.
- (24) Shekhah, O.; Wang, H.; Kowarik, S.; Schreiber, F.; Paulus, M.; Tolan, M.; Sternemann, C.; Evers, F.; Zacher, D.; Fischer, R. A.; et al. Step-by-Step Route for the Synthesis of Metal–Organic Frameworks. *J. Am. Chem. Soc.* **2007**, *129*, 15118–15119.
- (25) Biemmi, E.; Scherb, C.; Bein, T. Oriented Growth of the Metal Organic Framework Cu<sub>3</sub>(BTC)<sub>2</sub>(H<sub>2</sub>O)<sub>3</sub>·xH<sub>2</sub>O Tunable with Functionalized Self-Assembled Monolayers. *J. Am. Chem. Soc.* **2007**, *129*, 8054–8055.
- (26) Betard, A.; Fischer, R. A. Metal–Organic Framework Thin Films: From Fundamentals to Applications. *Chem. Rev.* **2012**, *112*, 1055–1083.